# Numerical and Analytical Study of 6H-SiC Detectors with High UV Performance

G. Brezeanu , M.Badila
*POLITEHNICA Univ. Bucharest, Romania, brezeanu@mcma.pub.ro*

F.Udrea, A.Mihaila, G.Amaratunga
*Cambrige University, UK fu@end.cam.uk*

J. Millan, P. Godignon
*CNM Barcelona, Spain josemillan@cnm.es*

## Abstract

*The paper is concerned with on the investigation of the UV detection performances of 6H-SiC Schottky and junction barrier diodes with oxide ramp termination . The devices exhibit a high responsivity in UV spectral range with excellent visible rejection ratio. An accurate model for the determination of the quantum efficiency is developed. Excellent agreement between model and simulated data is achieved. For transient photoresponse to a pulse light we found that Schottky diodes are superior to pn devices with the same parameters.*

## 1. Introduction

A wide range of applications such as aerospace, medical, biological and spectroscopic require optical semiconductor sensors with high ultraviolet (UV) responsivity, insensitive to direct solar radiation [1-3]. SiC is a good candidate for visible blind UV detectors due to its wide bandgap [2-3]. The development of UV sensors based on SiC devices is very attractive because it combines the high temperature capability with superior radiation hardness [2-3].The photodetectors are, usually, Schottky or *pn* junction diodes reverse biased. For SiC diodes we had previously proposed a simple planar edge termination based on a field plate overlapping on oxide ramp at the periphery of the contact [4-5]. We have proved experimentally the use of this termination on 4H-SiC and 6H-SiC for high voltage Schottky barrier diodes (SBDs) [4] and for *pn* junction barrier diodes (JBDs) [5].

Extensive Medici simulations have been carried out to demonstrate the excellent UV detection sensitivity of SiC SBD's and JBD's employing the oxide ramp termination. A modification of the analytical model for the detection quantum efficiency from the well-known Sze monograph [1] is also proposed in this paper.

## 2. Structure

Both SBD's and JBD's samples were fabricated on the same $nn^+$ 6H-SiC wafer using the same mask set and processing tools. Two insulating layers comprised of an undoped oxide layer and an 8% phosphorus doped oxide layer, with a total thickness of 1μm, were grown onto the epilayer. In order to obtain an oxide ramp profile a two steps wet etching were used: an initial etching in a standard oxide etch solution followed by an over-etching in a P-etch solution. Experimental measurements indicate that a ramp angle of less than $4^\circ$ was achieved. This low ramp assures a near ideal parallel-plane breakdown [4-5].

The $p^+$ layer of JBD's, with a thickness of 0.15 μm, was formed by Al implantation. 140 Å Pt was deposited and patterned, by lift-off, as Schottky contact on SBD's and as the ohmic contact on $p^+$ layer for JBD's.

Fig.1 shows reverse characteristics measured on SBD's. We can distinguish primarily two groups of diodes. The leakage current of one group increases with the increase in the reverse bias, a typical behaviour for unannealed Schottky contact. The other group of devices exhibits a low reverse current up to 500V. These diodes are recommended for photodetectors [5].

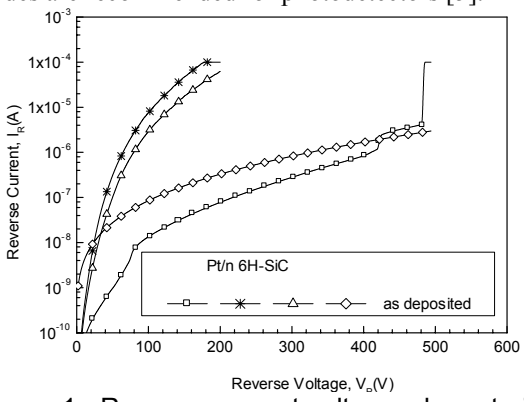


Figure 1. Reverse current-voltage characteristics measured on Pt/n 6H-SiC Schottky photodiode.

## 3. Quantum efficiency

One of the most important parameters for photodiodes is the quantum efficiency. This parameter is defined as the number of carriers generated per incident photons:

$$\eta = \frac{\Phi_{ph}}{\Phi_i} = \frac{J_{ph}/q}{J_i/q} = \frac{J_{ph}}{J_i} \qquad (1)$$

where $J_{ph}$ is the photogenerated current density by the absorbtion of the incident photon flux $\Phi_i$ (corresponding to a incident current density of $J_i$ ). Light absorbtion in semiconductor produces hole-electron pairs in the

depletion region or in the neutral bulk, within a diffusion length of it. The generation rate at a distance $x$ to the semiconductor is given by:

$$G(x)=(1-r)\Phi_i\alpha\cdot e^{-\alpha\cdot x} \quad (2)$$

where $r$ is the reflection coefficient.

Under steady-state conditions the total photocurrent density has two components:

$$J_{ph}=J_{dr}+J_{diff} \quad (3)$$

Here $J_{dr}$ is the drift current density due to carriers generated inside the depletion region which can be written as:

$$J_{dr}=q\int_0^{x_d}G(x)dx=q\Phi_i(1-r)(1-e^{-\alpha\cdot x_d}) \quad (4)$$

where $x_d$ is the depletion layer width.

The diffusion current density ($J_{diff}$) is given by:

$$J_{diff}=-qD_p\left.\frac{dp_n}{dx}\right|_{x=x_d} \quad (5)$$

Here $D_p$ is the diffusion coefficient for holes and $p_n$ is the hole density in the bulk of semiconductor considered to $n$-type. For $x> x_d$ the hole density (which are the minority carriers) is determined by the one dimensional diffusion equation:

$$D_p\frac{d^2p_n}{dx^2}-\frac{p_n-p_{n_0}}{\tau_p}+G(x)=0 \quad (6)$$

where $\tau_p$ is lifetime of excess holes and $p_{n_0}$ the equilibrium hole density. The solution of this equation is obtained using the following boundary conditions :

$$p_n(x_d)=G(x_d)\tau_p\,;\qquad p_n(\infty)=p_{n_0} \quad (7)$$

The diffusion current density is deduced as:

$$J_{diff}=(1-r)q\Phi_i\frac{\alpha^2L_p^2}{1+\alpha L_p}e^{-\alpha\cdot x_d} \quad (8)$$

with $L_p=\sqrt{D_p\tau_p}$ , which is holes diffusion length.

The quantum efficiency can be obtained from equations (1),(3),(4) and (8):

$$\eta=(1-r)\left[1-\left(1-\alpha L_p+\frac{\alpha L_p}{1+\alpha L_p}\right)e^{-\alpha\cdot x_d}\right] \quad (9)$$

Note that in [1] one obtain for the quantum efficiency the formula:

$$\eta=(1-r)(1-\frac{e^{-\alpha\cdot x_d}}{1+\alpha L_p}) \quad (10)$$

This is because a less accurate boundary condition at the edge of the depletion region is used: $p_n(x_d)=0$, see equation (7).

A related figure of merit for detectors is the spectral responsivity, which is the ratio of the photocurrent to the incident optical power [1]:

$$R=\frac{J_{ph}}{P_i}=\frac{J_{ph}/q}{\Phi_i}\cdot\lambda\cdot\frac{q}{hc}=\frac{\eta\lambda(nm)}{1{,}24} \quad (11)$$

where $\lambda$ is expressed in [$nm$] and $R$ result in [$mA/W$]. Therefore for a given quantum efficiency, the responsivity increases linearly with wavelength.

The photodiode absorbs radiation similar to a cut-off filter. The wavelength cut-off ($\lambda_c$) is established by the energy band of the semiconductor [1]. In the case of 6H-SiC material $\lambda_c=0.41\ nm$. Bearing in mind that the energy of photons decreases with increasing wavelength and that, for $\lambda>\lambda_c$, the photocurrent decreases abruptly it can be understood that the curve of the spectral responsivity versus wavelength in the ideal case has a triangular shape.

## 4. Results. Discussion

The MEDICI program was used to numerically simulate the photoresponse in UV spectral range of 6H-SiC SBD's and JBD's with oxide ramp termination having different epilayer parameters ($N_d$ / $x_e$).

The performances for a uniform illumination (with a monochromatic light flux of $10^{20}$ $cm^{-2}s^{-1}$) are shown in Figs.2-5. The quantum efficiency is almost flat over the spectral range from 250 to 350 nm (Fig.2). The responsivity increases linearly over the above-mentioned spectral range (Figs.3). The highest responsivity (over 200 mA/V) is obtained at 350 nm, which corresponds to a quantum efficiency of about 75%. $R$ increases with the increase in the bias voltage up to 10V and also with the decrease in the doping of the $n$-epilayer (Fig.3b). A weak dependence of the photoresponse with the epilayer thickness and with the increase in the reverse bias over 10V can be observed (Figs.2-4). At a low doping of epilayer the bias effect is also reduced.

Above wavelengths of 350 nm the responsivity and quantum efficiency decreases abruptly (Figs.2-3). The rejection factor, defined as the ratio between the maximum responsivity and $R$ value at cut-off wavelength ($\lambda_c$ =410nm) is greater than 10. This demonstrates the high visible blind performance of the photodetectors with oxide ramp termination.

Similar behaviour are achieved on SBD's and JBD's with the same epilayer (Figs.3-4).

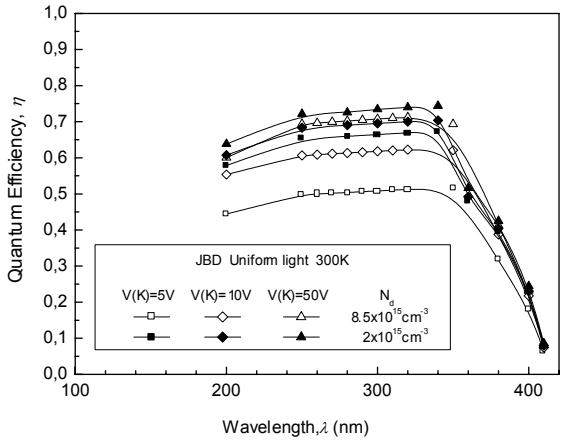


Figure 2. The quantum efficiency vs. wavelength plots for several biases of JBD's with two epilayer doping ($x_e$=8 μm).

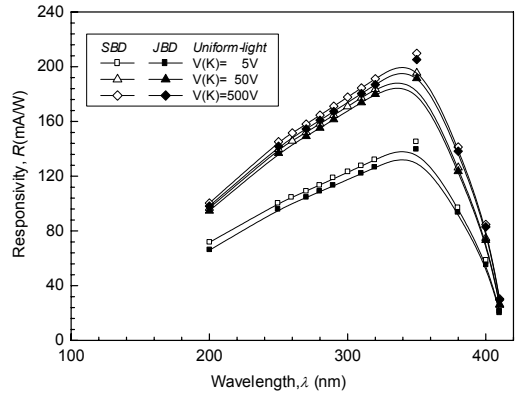


(a)

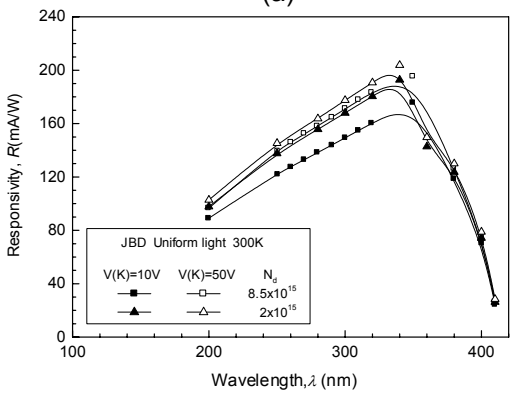


(b)

Figure 3. Spectral responsivity versus wavelength for several reverse biases of: (a) SBD's and JBD's with the same n-epilayer, and (b) JBD's with different *n*-epilayer parameters.

The quantum efficiency is analysed in the following more detail. The model used includes the reflection at the air-SiC interface. The reflection coefficient is:

$$r = \left( \frac{n_{sic} - n_0}{n_{sic} + n_0} \right)^2 \tag{12}$$

For $n_{SiC} = 2.7$ and $n_0 = 1$ which are the indices of reflection of SiC and air, respectively, result in $r=0.21$.

The absorption coefficient as a function of photon wavelength between 200 and 400nm is calculated using:

$$\alpha = 3400 \left( \frac{1241.5}{\lambda} - E_g \right)^2 \tag{13}$$

where $\lambda$ is in [$nm$]. $E_g$ is the bandgap energy of 2.97 eV.

In Fig.4 the simulated data of the quantum efficiency are compared with the calculated curves using equations (9) and (10) , respectively.The dependence of $\eta$ on the reverse bias can be explained taking into account the voltage dependence of the depletion region width ( $x_d$ ). For a Schottky diode or a *pn* diode with a one sided abrupt junction $x_d$ is given by:

$$x_d = \left( \frac{2\varepsilon}{qN_d} (V(K) + V_{bi}) \right)^{1/2} \tag{14}$$

where $\varepsilon$ is SiC permittivity, $V_{bi}$ is built-in potential and *V (K)* the diode reverse voltage.

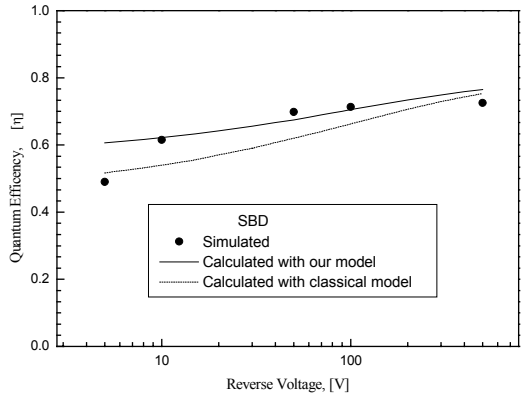


(a)

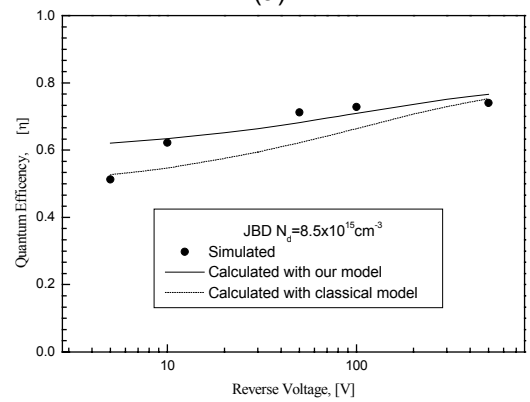


(b)

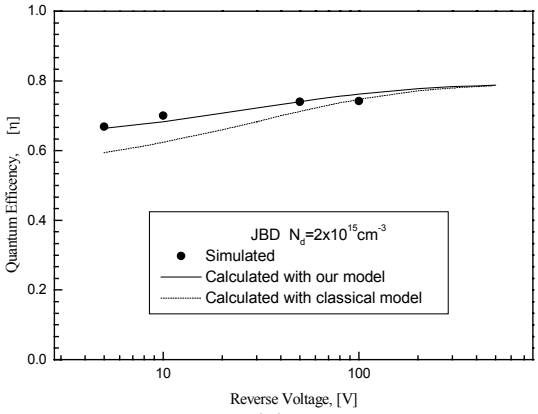


(c)

Figure 4. Simulated (symbols) and calculated (curves) quantum efficiency versus reverse voltage of: (a) SBD's ($N_d$=8.5x10$^{15}$cm$^{-3}$) and (b),(c) JBD's.

An excellent agreement of the the simulated data with calculated plots using our model is evidenced in Fig.4. The only fitting parameter is the hole diffusion length in the *n* base. The best fit was obtained for a lengths of 4.45μm and 4.55μm which corresponds to a base doping of 8.5x10$^{15}$ and 2x10$^{15}$cm$^{-3}$, respectively. A relatively poor fitting to the simulated data is observed for the classical model.

In Fig.5 the dependence of the responsivity on the photon flux is shown. The photoresponse of both SBD's and JBD's biased over 10V is found to be practically independent of the $\Phi_i$ from $10^{17}$ to $10^{20}$ cm$^{-2}$s$^{-1}$. A

slightly decrease of $R$ at low reverse voltage only for devices with epilayer doping of 8.5 x$10^{15}$ $cm^{-3}$ can be observed at high photon flux. This decrease explains the small differences between the simulated data and calculated plots of the quantum efficiency that can be seen on Fig.4 (a, b), for $V(K)$=5V and $N_d$=8,5×$10^{15}$$cm^{-3}$ .

The dynamic behaviour of the photodetectors with oxide ramp termination was also investigated. For this

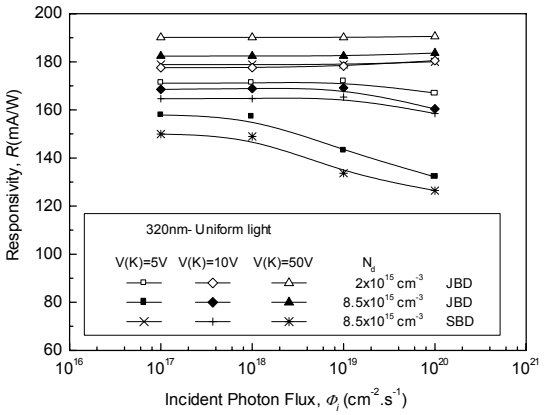


Figure 5. Responsivity of SBD's and JBD's versus incident photon flux for different biases (λ=320nm).

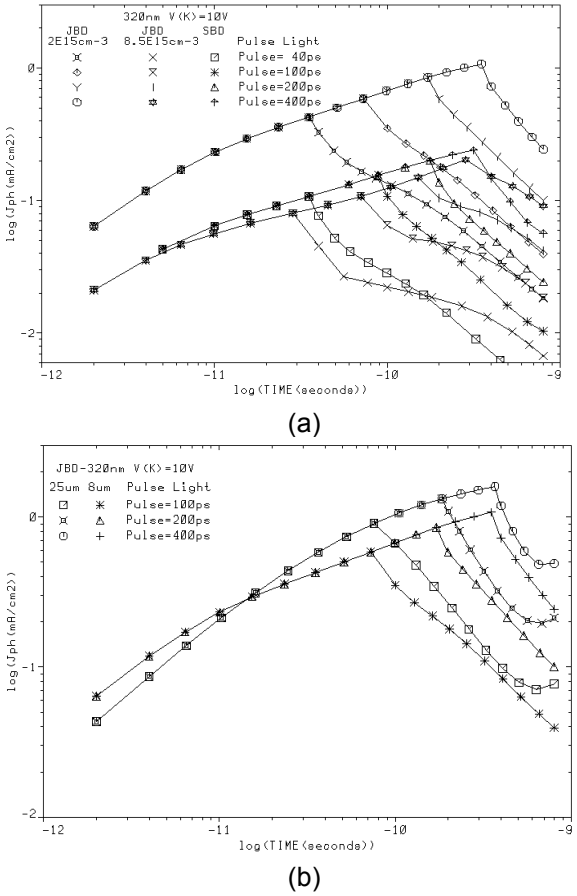


Figure 6. Comparison of the transient photoresponse for both: (a) SBD's and JBD's with the same epilayer, (b) JBD's with two thickness of epilayer ($N_d$=2×$10^{15}$ $cm^{-3}$).

the operation of the photodetector under pulse light exposure with various duration has been simulated; so that the transient time can be determined (Fig.6).

The transient response of SBD's is superior to that obtained in a similar JBD structures . The effect of the photodiode bias voltage is more important for uniform illumination. Also photocurrent decay rate increase at high reverse biases (Fig.6).

The response speed is limited by a combination of two factors: diffusion of carriers generated in the neutral regions and drift time in the depletion region [1]. The transient time in the depletion region and the necessary time of the carriers generated outside the depletion region to diffuse to junction explain the considerable time delay between the time end of the pulse and the time at which the current reaches its maximum value. This delay is shorter in SBD's and JBD's with lower epilayer doping due to the diffusion effects in *n* neutral and *p* neutral regions, respectively.

## 5. Conclusions

In this paper we demonstrate that the oxide ramp termination is highly suitable for UV photodetectors. The main detection parameters, quantum efficiency and responsivity have been analysed in detail for SBD's and JBD's with various epilayers. The response to a pulse light excitation has been also investigated. Owing to higher photocurents and higher speed, SBD's are strong candidate to JBD's for UV transient detection.

A new analytical model to evaluate quantum efficiency is also presented and discussed. The very good agreement between calculated curves and simulated data confirm the proposed model.

## 6. References


[1] S. M. Sze *Physics of Semiconductor Devices,* J.Wiley & Sons, New-York ,1981.

[2] T. Toda, Y. Ueda, M. Sawada, "Lowering the Annealing Temperature of Ni/SiC for Ohmic Contacts under $N_2$ Gas, and Application to a UV Sensor", *Mat.Science Forum,* vol. 338-342(2000) pp.989-992.

[3] J.T. Torvik, J.I. Pankove and B.J. Van Zeghbroeck, "Comparison of GaN and 6H-SiC pin photodetectors with excellent UV sensitivity and selectivity", *IEEE Trans. Electron. Dev.*, vol. 46 (1999), pp.1326-1331.

[4] G. Brezeanu, M. Badila, B. Tudor, J. Millan, P. Godignon, F. Udrea, G. Amaratunga, and A. Mihaila, "Accurate Modelling and Parameter Extraction for 6H-SiC Schottky Barrier Diodes (SBD's) with Nearly Ideal Breakdown Voltage", *IEEE Trans. Electron. Dev.*, vol. 48 (2001), pp.2148-2153.

[5] G. Brezeanu, M. Badila, P. Godignon, J. Millan, F. Udrea, A. Mihaila, G. Amaratunga "An Effective High Voltage Termination for SiC Planar pn Junctions for Use in High Voltage Devices and UV Detectors", *Technical Digest of ICSCRM-2001*, Tsukuba, Japan,pp.175-176.